Biochemistry

 Volume 37, Number 8 February 24, 1998

Accelerated Publications

In Bacterial Reaction Centers, a Key Residue Suppresses Mutational Blockage of Two Different Proton Transfer Steps†

Jaroslava Miksovska,*,‡ Marie Valerio-Lepiniec,*,‡ Marianne Schiffer,§ Deborah K. Hanson,§ and Pierre Sebban‡

Centre de Génétique Moléculaire, CNRS, Bât. 24, 91440 Gif sur Yvette, France, and Center for Mechanistic Biology and Biotechnology, Argonne National Laboratory, 9700 South Cass Avenue, Argonne, Illinois 60439

Received October 30, 1997; Revised Manuscript Received January 7, 1998

ABSTRACT: In reaction centers of *Rhodobacter* (*Rb.*) *capsulatus*, the M43Asn → Asp substitution is capable of restoring rapid rates for delivery of the second proton to Q_B in a mutant that lacks L212Glu. Flash-induced absorbance spectroscopy was used to show a nearly native rate for transfer of the second proton to Q_B ($\cong 700\ s^{-1}$) in the L212Gln+M43Asp double-mutant reaction center; this rate was shown to decrease more than 1000-fold in the photoincompetent L212Glu → Gln mutant [Miksovska, J., Kálmán, L., Maróti, P., Schiffer, M., Sebban, P., and Hanson, D. K. (1997) *Biochemistry 36*, 12216−12226]. In *Rb. sphaeroides*, the equivalent M44Asn → Asp mutation was reported to restore the rate of transfer of the first proton to a wild-type level when it is added to the L213Asp → Asn photoincompetent mutant [Rongey, S. H., Paddock, M. L., Feher, G., and Okamura, M. Y. (1993) *Proc. Natl. Acad. Sci. U.S.A. 90*, 1325−1329]. It is remarkable that the same second-site mutation can compensate for both of these mutations which severely impair reaction center function by blocking two different proton-transfer reactions. We suggest that residue M43Asp is situated in a key position which can link pathways for delivery of both the first and second protons (involving structured water molecules) to Q_B.

Bacterial reaction centers convert electromagnetic light energy into chemical free energy by catalyzing a transmembrane charge separation between a primary electron donor (P) and a system of quinone electron acceptors (Q_A and Q_B). These cofactors are bound within a complex of three transmembrane polypeptide chains, designated L, M, and H; the structure is known to nearly atomic resolution for the reaction centers of *Rhodopseudomonas* (*Rps.*) *viridis* (*1*) and *Rhodobacter* (*Rb.*) *sphaeroides* (*2*−*7*). P is a dimer of bacteriochlorophyll, which is situated near the periplasmic side of the complex, and the quinones are located near the cytoplasmic side. The primary quinone Q_A functions as a one-electron acceptor and is reoxidized by electron donation to the secondary quinone Q_B in 5−200 μs (*8*−*10*). At variance to Q_A, Q_B accepts two electrons and two protons in a sequential process.

The identification of the intraprotein pathways for the delivery of protons to Q_B has been the motivation for many experimental investigations (for reviews, see 11−13). In reaction centers of *Rb. sphaeroides* and *Rb. capsulatus*, it has been established that residue L213Asp, located ∼5 Å from Q_B, has an important electrostatic and/or structural role in delivery of the first proton to Q_B^-. Indeed, the replace-

† Supported by the Human Frontier of Science Organization RG-329-95M, by the CNRS, and by the U.S. Department of Energy, Office of Health and Environmental Research, under Contract W-31-109-ENG-38.

* J.M. and M.V.-L. contributed equally to this work.
‡ CNRS.
§ Argonne National Laboratory.

S0006-2960(97)02696-2 CCC: $15.00
Published on Web 02/05/1998

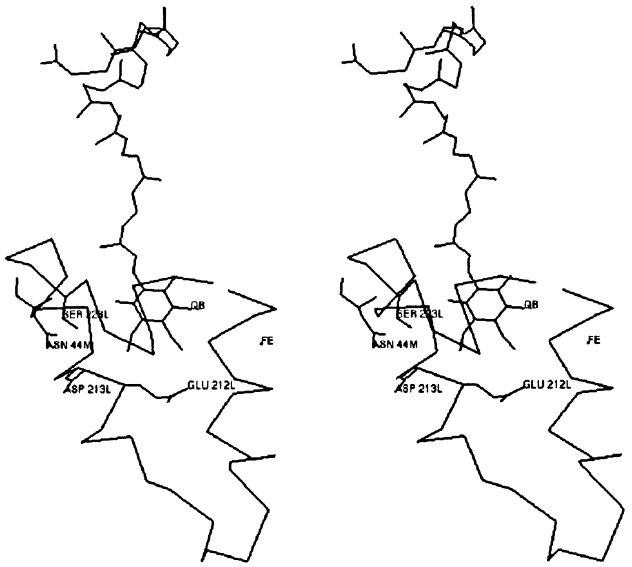

FIGURE 1: Stereoview of a slice of the reaction center structure (dark) from *Rb. sphaeroides* determined by Stowell et al. (*2*). The plane of the membrane is horizontal. This figure shows the carbon backbone of the Q_B binding pocket (residue range L190−L230) and the side chains of the M44Asn, L212Glu, L213Asp, and L223Ser residues. This figure was achieved using the "Turbo-Frodo" program (from Biographics).

ment of L213Asp by Ala or Asn yields a photoincompetent strain whose reaction center is severely impaired in transfer of the first proton to Q_B^- (*14*−*16*). Very interestingly, efficient delivery of the first proton to this acceptor is totally restored in the L213Asp-M44Asn → Asn-Asp double mutant of *Rb. sphaeroides* (*17*); the equivalent mutation, M43Asn → Asp, occurs as an intergenic suppressor which restores function to *Rb. capsulatus* reaction centers carrying the engineered L212Glu-L213Asp → Ala-Ala mutations (*18*). In the case of this Ala-Ala double mutant, it is clear that the M43Asp (M43D) substitution is compensating for the loss of L213Asp rather than L212Glu, since the L212Glu → Ala mutant is photocompetent (*19*, *20*). The M43(M44)Asn → Asp mutation increases the negative electrostatic environment of Q_B^- (*16*, *17*, *21*). On the basis of the comparison with *Rps. viridis*, whose reaction centers contain an Asn at position L213 and an Asp at position M43 (∼9−11 Å from either of the carbonyl groups of Q_B), the above observations suggested that the Asp ↔ Asn combination in positions L213 ↔ M44 (M43) (see Figure 1) is a functional requirement.

In wild-type reaction centers of *Rb. sphaeroides* and *Rb. capsulatus*, delivery of the second proton to Q_B has been shown to involve L212Glu (∼6 Å from Q_B); its replacement by Gln results in a photosynthetically incompetent strain (*20*, *22*−*25*). Since the M43Asn → Asp mutation can restore first proton transfer to L213 mutants, we decided to test the hypothesis that it might also restore second proton transfer and thus compensate for the L212Glu → Gln mutation. We therefore constructed the L212Q+M43D double-mutant strain, and it is photocompetent. We have analyzed the electron- and proton-transfer capabilities of its reaction centers. We compare them to those that were previously reported for the reaction centers of the L212Q mutant and the wild-type *Rb. capsulatus* (*25*). We show here that the reaction center of the L212Q+M43D mutant has indeed recovered the ability to transfer the second proton to Q_B^- at a rate that is rapid and is comparable to that of the wild type.

MATERIALS AND METHODS

Mutant Construction. For all strains, the *Rb. capsulatus* deletion strain U43 (LHI^-, $LHII^-$, RC^-; *26*) was complemented by derivatives of broad-host-range plasmid pU2922 (*27*); the wild-type is LHI^+, $LHII^-$, RC^+. Construction of the L212Q mutant was previously described (*28*). To link the M43Asn → Asp mutation to the L212Q mutation, an intermediate plasmid was constructed in which a *Bgl*II-tagged M-gene segment was ligated to the L-gene segment carrying the site-specific L212Glu → Gln mutation. For the double mutant, the M-gene segment was excised from the plasmid isolated from the L212Ala-L213Ala-M43Asp suppressor strain (*18*); it was then used to replace the *Bgl*II-tagged M gene in the above intermediate plasmid. Constructs were verified by screening small-scale plasmid preparations for loss of the *Bgl*II site. The L212Q-M43D double-mutant plasmid was then transferred to U43 by conjugation with *E. coli* strain S17-1 (*29*).

Biochemical Preparations. The L212Q+M43D, L212Q, and wild-type strains were grown under chemoheterotropic conditions (dark, semiaerobic) at 34 °C on RPYE medium containing 30 μg/mL kanamycin to ensure the presence of the plasmid (*30*). Reaction centers were prepared as previously described (*31*).

Electron-Transfer Measurements. The kinetics of $P^+Q_A^-$ and $P^+Q_B^-$ charge recombination were measured at 430 nm. The first electron-transfer kinetics were measured by monitoring the electrochromic band shift of the bacteriopheophytin at 751 nm (*9*). The second electron-transfer kinetics were detected at 450 nm (*32*, *33*), in the presence of 20−40 μM cyt *c* (Sigma) reduced by 250−500 μM sodium ascorbate. Reconstitution of the Q_B site was achieved by the addition of ∼50−75 μM UQ_6. In the L212Q and the L212Q+M43D mutants, occupancies of the Q_B site were restored to ∼80% and ∼70%, respectively, as measured by the relative amplitude of the slow ($P^+Q_B^-$) phase of charge recombination and by the amplitude of cytochrome oxidation after the second flash versus the first one ($\Delta A_2/\Delta A_1$).

Proton-Transfer Measurements. The kinetics of proton uptake were determined at pH 7.5 by measuring the absorbance changes at 585 nm (isosbestic point of the P^+ absorbance changes) of the pH-sensitive dye *o*-cresol red. The assay solution routinely contained 1−2 μM reaction centers, 50 mM NaCl, 0.03% Triton X-100, 100 μM ferrocene, 500 μM potassium ferrocyanide, 60 μM UQ_6, and 40 μM *o*-cresol red. The reaction centers were extensively dialyzed in order to keep the buffer concentration below 5−10 μM. The calibrations of the stoichiometries of proton uptake were performed by additions of known amounts of HCl (1 M stock; Merck). The net proton uptake was obtained by subtracting the buffered signal from the unbuffered signal.

RESULTS AND ANALYSIS

The pH Dependence of the $P^+Q_B^-$ Charge Recombination Reaction. The pH dependence of the rate constant (k_{BP}) of the $P^+Q_B^-$ charge recombination reaction that was measured

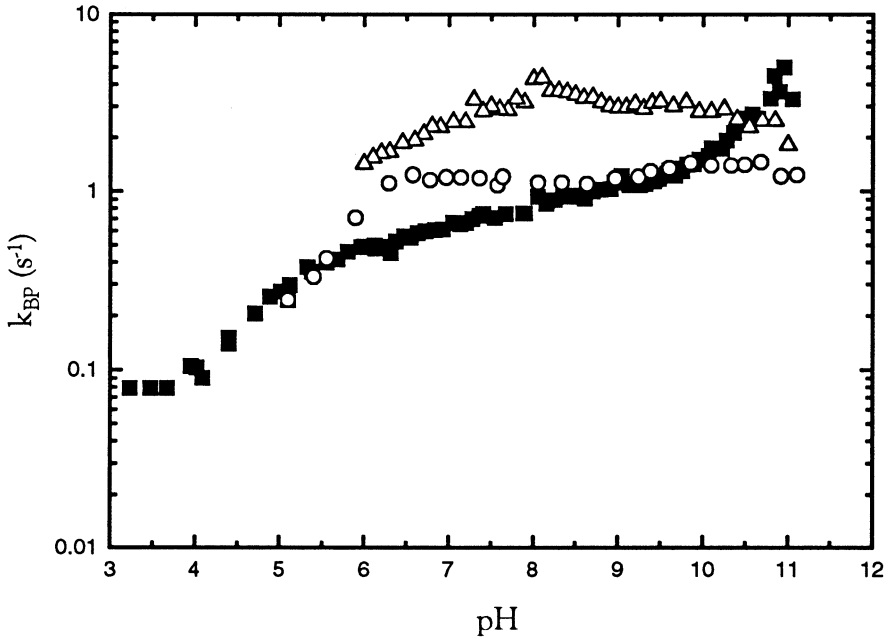

FIGURE 2: pH dependencies (measured at 430 nm) of the rate of $P^+Q_B^-$ charge recombination in the reaction centers (1 μM) from the L212Q+M43D (△) and L212Q (○) mutants and from the wild type (■). Conditions: 0.05% LDAO or 0.03% Triton X-100, buffers depending on pH as indicated in the text, 50−75 μM UQ_6 added, 21 °C.

for the L212Q+M43D mutant reaction centers is presented in Figure 2. Previously reported measurements for wild-type and L212Q mutant reaction centers are also shown (*25*). At pH 8, k_{BP} is increased 4−5-fold in the L212Q+M43D mutant ($k_{BP} \cong 4\ s^{-1}$) compared to the reaction centers of the wild type ($k_{BP} \cong 0.83\ s^{-1}$) and the L212Q mutant ($k_{BP} \cong 1\ s^{-1}$). The rate constants ($k_{AP}$) of the $P^+Q_A^-$ decay kinetics measured at pH 8 for the L212Q and L212Q+M43D mutants are about 6.7 s^{-1} (data not shown), slightly smaller than in the wild type. Therefore, the data of Figure 2 suggest that the replacement of M43Asn by Asp decreases the free energy gap [$\Delta G°_{AB} = -kT \ln(k_{AP}/k_{BP} - 1)$] (*34*) between the Q_A^- and Q_B^- states in the L212Q+M43D double mutant by about 33 meV at neutral pH compared to the L212Q mutant. This value is consistent with the previously reported electrostatic effect of the M43Asn → Asp single mutation, which reduced $\Delta G°_{AB}$ by about 25 meV in comparison to the wild-type *Rb. capsulatus* (*21*). Similar to previous observations for the L212Q mutants of both *Rb. capsulatus* (*25*) and *Rb. sphaeroides* (*22*), the notable acceleration of k_{BP} at high pH which is seen in the wild type is not observed in reaction centers of the L212Q+M43D mutant. Instead, a slight but continuous decrease of k_{BP} from 3.3 to 2.5 s^{-1} is measured in this mutant in the pH range 8−11.

pH Dependence of the Rate Constant for Transfer of the First Electron from Q_A^- to Q_B. The pH dependencies of the rate constants [$k_{AB}(1)$] of the first electron transfer from Q_A^- to Q_B, measured for the wild-type, L212Q, and L212Q+M43D reaction centers at 751 nm, are presented in Figure 3. This is the first report of the pH dependence of $k_{AB}(1)$ for wild-type reaction centers of *Rb. capsulatus*. Up to pH 9, the pH titration curve of $k_{AB}(1)$ is essentially flat with a value of about 11 500 s^{-1}. Above this pH value (apparent p$K_a \cong 9.1$), $k_{AB}(1)$ decreases linearly with a slope of nearly $-1\ H^+/e^-$ to reach a value of 530 s^{-1} at pH 10.25. The magnitude of the slope observed for $k_{AB}(1)$ above the apparent pK_a suggests a diffusion process for protons that is similar to that seen in water. The shape of this curve is comparable to previously reported data for *Rb. sphaeroides* reaction centers (*22*, *23*), but *Rb. capsulatus* reaction centers display slightly higher values for $k_{AB}(1)$. In both of the above species, the first electron-transfer process is multiphasic with rates ranging between ∼4 μs and 2 ms (*9*, *10*). We did not observe such heterogeneity even in the blue region of the semiquinone spectra (460 nm) in the *Rb. capsulatus* reaction centers. Our instrumental response time (2−3 μs) might be limiting if faster components are present. This possibility is under further investigation.

The pH dependence of $k_{AB}(1)$ is different in the L212Q mutant where it remains nearly constant in the pH range 8−10. At pH 8, the $k_{AB}(1)$ values for the L212Q and L212Q+M43D mutants are about the same, 4500 s^{-1}; this value is reduced only ≅2.5-fold from that of the wild type. After showing a constant pH dependence from pH 7.25−8.0, $k_{AB}(1)$ for the L212Q+M43D mutant decreases continuously above pH 8, with a slope of approximately $-0.33\ H^+/e^-$. At pH 10, the $k_{AB}(1)$ values for the wild type and the L212Q+M43D mutant are nearly equivalent.

pH Dependence of the Rate of the Second Electron-Transfer Reaction, $k_{AB}(2)$. The pH dependence of $k_{AB}(2)$ measured for the L212Q+M43D mutant reaction centers is presented in Figure 4; previously measured values for the wild type and the L212Q mutant (*25*) are also shown. In the pH range 7.5−9, $k_{AB}(2)$ is approximately the same, within the experimental error, for all three reaction centers. At pH 8, $k_{AB}(2)$ is about 1000 s^{-1} in the L212Q+M43D strain, 1200 s^{-1} in the L212Q, and 1800 s^{-1} in the wild type. However, the pH dependence of $k_{AB}(2)$ is different in the L212Q+M43D reaction center. The slope of the pH dependence for $k_{AB}(2)$ in the L212Q+M43D mutant is smaller than the two other strains studied. In addition, the pH titrations of $k_{AB}(2)$ in the wild type and the L212Q mutant display a breakpoint at pH ∼ 9. No such break is observed for the L212Q+M43D mutant.

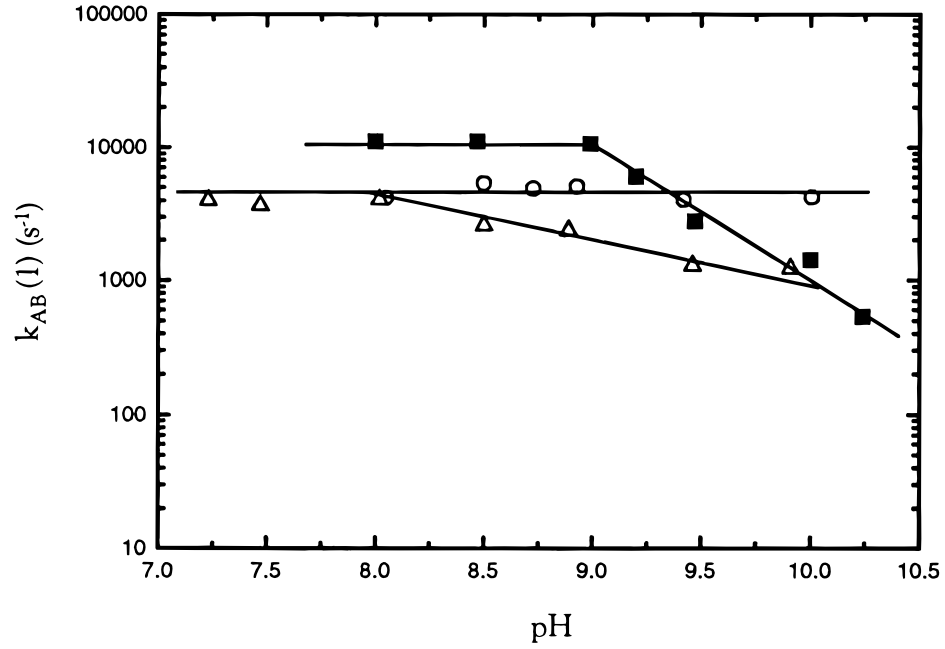

FIGURE 3: pH dependencies of the rate of first electron transfer from Q_A^- to Q_B in the reaction centers (~2 μM) from L212Q+M43D (△) and L212Q (○) mutants and from the wild type (■). Conditions as in Figure 2.

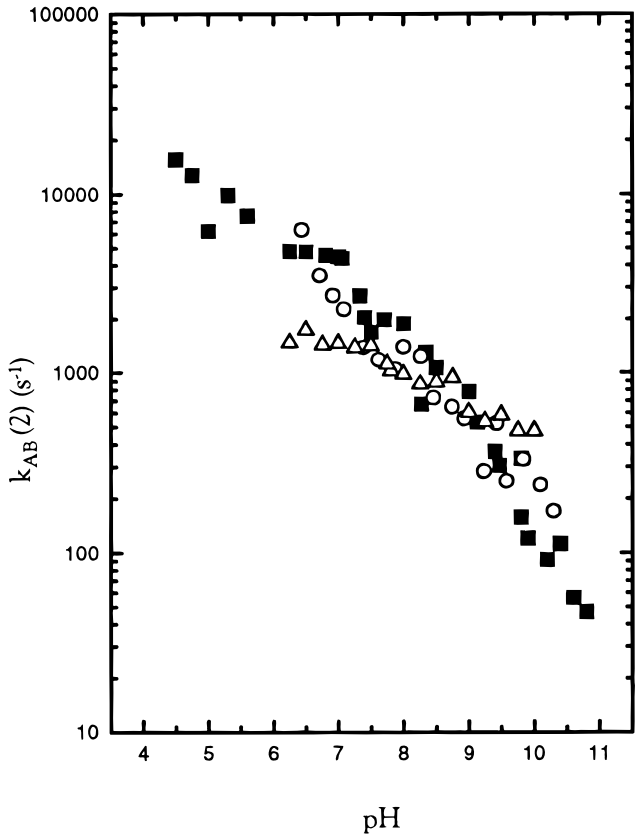

FIGURE 4: pH dependencies of the rate of second electron transfer in reaction centers (~2 μM) from the L212Q+M43D (△) and L212Q (○) mutants, and from the wild type (■). Conditions as for Figure 2, plus 40 μM cytochrome *c* and 200−500 μM ascorbic acid.

Multiflash Cytochrome c Oxidation. A convenient method for determining the rate-limiting steps for electron- and proton-transfer reactions is to observe the patterns of oxidation of exogenous cytochrome *c* (detected at 550 nm) following closely spaced saturating flashes. The results from an experiment conducted with a 40 ms flash interval are shown in Figure 5. As observed in this figure, a severe damping of the oxidations is detected in the L212Q mutant reaction centers after the third flash. A similar pattern was observed for the same mutant from *Rb. sphaeroides* (*22*). This type of behavior has previously been attributed to the inability of the reaction centers from this mutant to rapidly transfer the second proton to Q_B^- (*22*). The reaction centers from the L212Q mutant are therefore blocked in the $PQ_A^-Q_B^{2-}$ state after three photochemical events resulting in the oxidation of 3 cyt/RC. As shown in Figure 5, this damping is absent in the L212Q+M43D reaction centers where the amount of cytochrome *c* that is oxidized in steps 2−8 is equal. In the double mutant, the lower Q_B occupancy and lower $Q_A^- \leftrightarrow Q_B^-$ equilibrium constant cause the cytochrome oxidation steps to be slightly smaller than those seen for an equivalent concentration of wild-type reaction centers. This result suggests that, in comparison to the impaired L212Q mutant, the L212Q+M43D mutant can transfer the second proton to Q_B efficiently and rapidly.

Turnover of Exogenous Cytochrome c under Strong Continuous Illumination. To further verify the recovery of proton-transfer capabilities of the L212Q+M43D mutant, we have measured the rate of cytochrome turnover under strong continuous illumination. The data from this mutant are presented in Figure 6, together with previously measured rates for the wild-type and the L212Q mutant reaction centers (*25*). In the wild type, at pH 7.5, a rate of about 475 cyt_{ox}/RC/s was measured. In the L212Q reaction center, at the same pH, this rate is decreased to 28 cyt_{ox}/RC/s, because of the kinetic bottleneck for delivery of the second proton. Consistent with the data shown in Figure 5, the L212Q+M43D reaction center displays a much faster cytochrome turnover rate (≅ 220 cyt_{ox}/RC/s) than does that of the L212Q mutant.

Kinetics of Proton Uptake following the First and Second Flashes. To quantitatively measure the stoichiometry of and the kinetics for second proton transfer in the L212Q+M43D

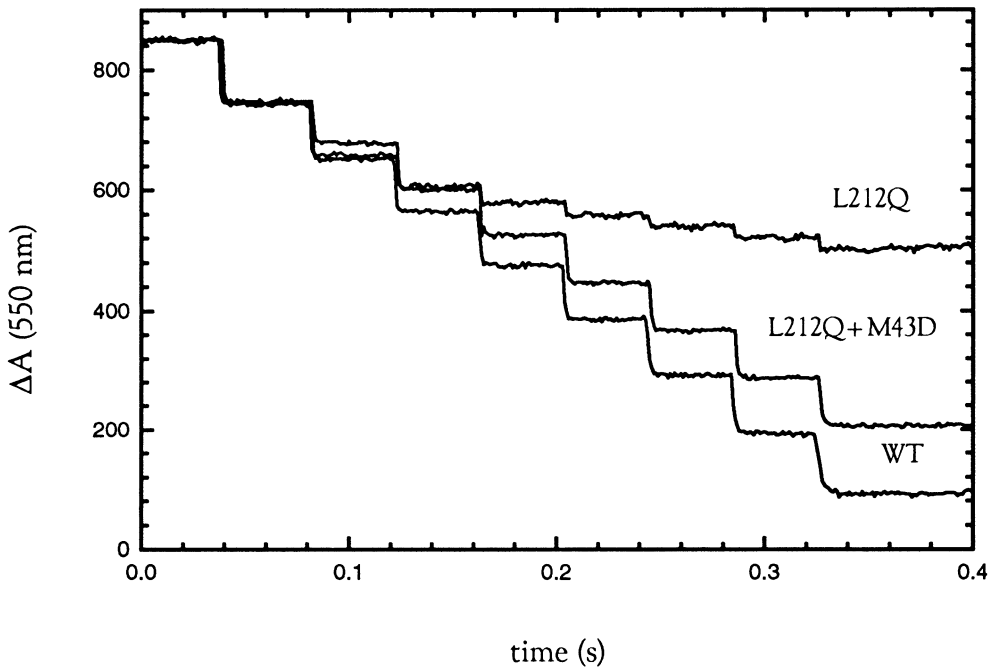

FIGURE 5: Multiflash cytochrome *c* oxidation pattern measured in the reaction centers (1 μM) from the L212Q+M43D and L212Q mutants and from the wild type. Conditions: 10 mM Tris, pH 7.8, 20 μM cytochrome *c*, 250 μM ascorbic acid, 75 μM UQ_6.

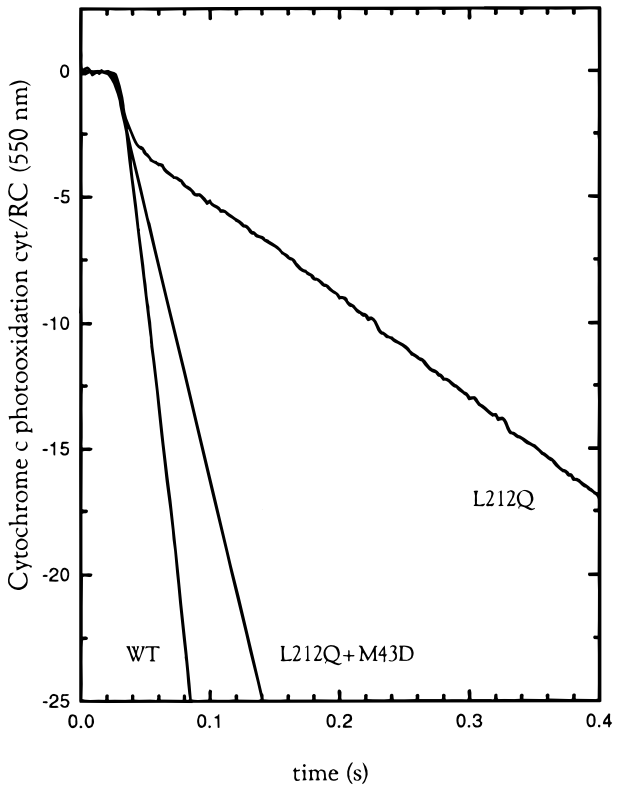

FIGURE 6: Rate of photooxidation of exogeneous cytochrome *c* under continuous illumination in reaction centers (1 μM) from the L212Q+M43D and L212Q mutants and from the wild type. Conditions: 10 mM Tris, pH 7.8, LDAO 0.05%, plus 20 μM reduced cytochrome *c*, 5 mM UQ_0; 550 nm.

reaction center, we have directly measured the absorbance changes of the pH-sensitive dye *o*-cresol red at pH 7.5 following two saturating flashes. The data for the L212Q+M43D mutant are shown in Figure 7, where they are compared to data previously reported for the reaction centers of the L212Q mutant and the wild type (*25*). In the wild type, after the uptake of a partial proton ($\sim$0.6 H^+) with the first flash, the full complement of two protons is reached by further proton uptake on a fast time scale ($\sim$950 s^{-1}) that occurs with the second flash. In the L212Q mutant, the kinetics of proton uptake with the second flash is notably slowed to about 0.66 s^{-1} reflecting very slow delivery of the second proton to Q_B. Remarkably, the addition of the M43Asn → Asp mutation restores a rapid rate for uptake of the second proton to the L212Q+M43D reaction centers (700 s^{-1}, data not shown), such that its rate is comparable to that of the wild-type. It is of interest to note that the amount of proton uptake that occurs with the first flash, i.e., uptake by the Q_B^- state, is nearly the same for the wild type and the two mutant reaction centers, therefore it does not involve L212Glu. This observation supports our previous suggestion that L212Glu is essentially protonated in wild-type reaction centers of *Rb. capsulatus* at neutral pH (*25*).

DISCUSSION

The reaction center of the L213Asp → Asn mutant is blocked at the critical stage of transfer of the first proton to Q_B^- (*17*, *23*); the L212Glu → Gln mutant is blocked for uptake of the second proton following formation of the Q_B^-(H) state (*22*, *23*, *25*). Either mutation yields a photosynthetically incompetent strain. Rongey et al. (*17*) showed that the M44Asn → Asp mutation could restore native rates for first proton transfer to the L213Asn-M44Asp double-mutant reaction center of *Rb. sphaeroides* (M43 in *Rb. capsulatus*). In this work, we show that the M43Asn → Asp mutation also has a major effect on the rate of transfer of the second proton, such that this reaction in the *Rb. capsulatus* L212Q+M43D double-mutant reaction center is rapid, occurring at a near-native rate.

It is clear that the primary effect of the M43Asn → Asp substitution, when it is coupled with the L212Q mutation, is to accelerate the second proton-transfer reaction. The rate of transfer of the first electron from Q_A^- to Q_B, measured at

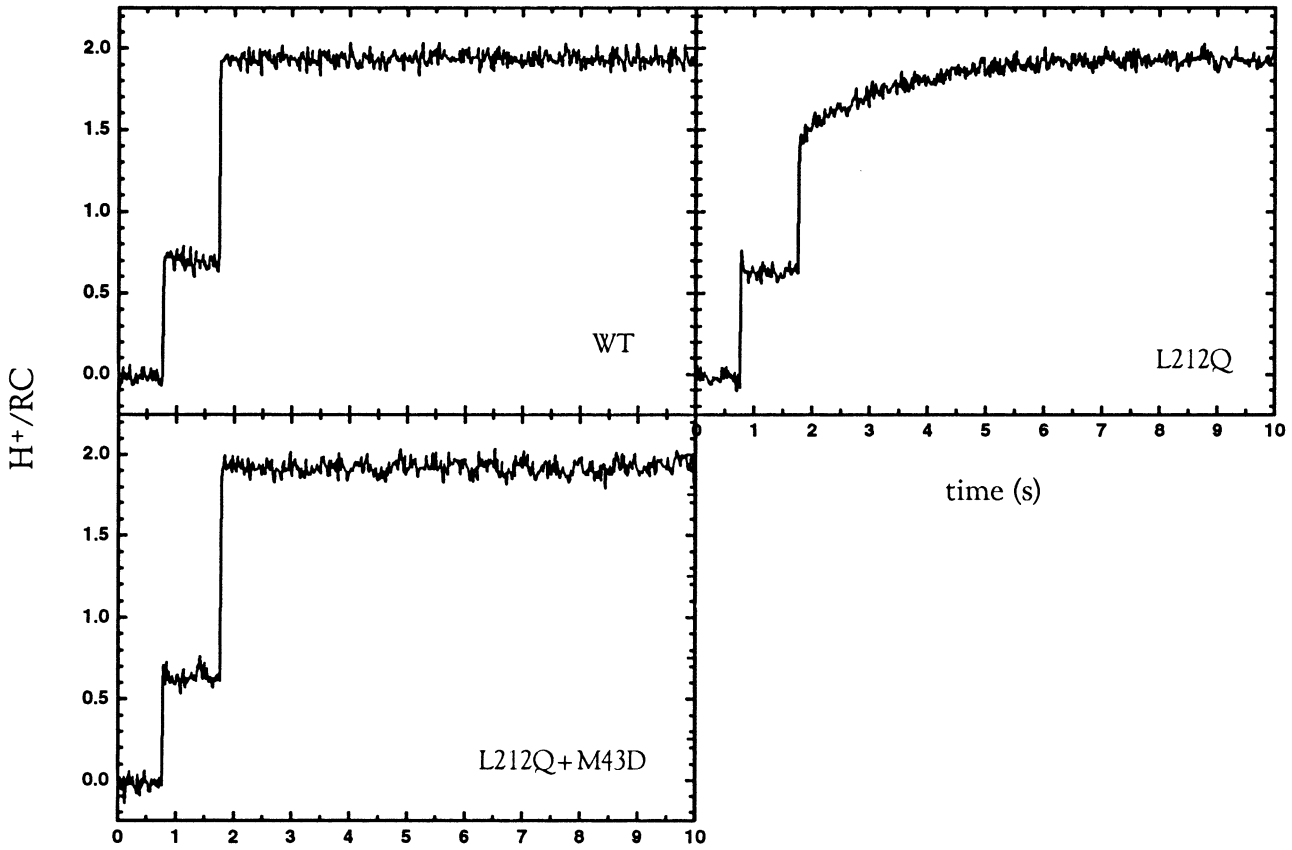

FIGURE 7: Stoichiometries and kinetics of proton uptake after the first and second flashes in reaction centers (~2 μM) from the L212Q+M43D and L212Q mutants and from the wild type. Conditions: 50 mM NaCl, 0.03% Triton X-100, pH 7.5, 100 μM ferrocene, 500 μM potassium ferrocyanide, 50−75 μM UQ_6, 40 μM *o*-cresol red; 585 nm. The net proton uptake was obtained by subtracting the buffered signal from the unbuffered traces.

pH 8, is the same in the L212Q and the L212Q+M43D mutant reaction centers, decreased only ~2.5 times from that of the wild type. The rate of the second electron transfer from Q_A^- to Q_B^- is essentially native in both mutant reaction centers. At variance, the multiflash cytochrome oxidation patterns as well as the measurements of the rates of cytochrome photooxidation turnover reveal a very different behavior for the L212Q mutant reaction center as compared to the L212Q+M43D mutant or the wild type. Finally, the direct measurements of the stoichiometries and kinetics of proton transfer after two flashes prove that the reaction centers of the L212Q+M43D mutant have the ability to transfer the second proton at a rate that is comparable to that of the wild type; this rate is more than 1000 times faster than that of the L212Q mutant.

It is remarkable that one substitution, M43Asn → Asp, is capable of restoring activity to reaction centers carrying mutations which affect two different protonation steps. It is likely that L213Asp has a structural role as a penultimate donor of the first proton to the O5 carbonyl of Q_B as well as its role in influencing the electrostatic environment of Q_B^-. To restore function so completely to reaction centers lacking L213Asp, M43Asp must be capable of assuming both roles. Because of their relative proximities in the light structure of the *Rb. sphaeroides* reaction center (*2*−*6*), the replacement of L212Glu by Gln probably causes a physical blockage in the movement of the second proton to the O2 carbonyl of Q_B because L212Glu can be effectively substituted by Ala in *Rb. capsulatus* (*25*); the blockage can be alleviated by the shorter side chain and the likely involvement of a water molecule. In the case of blockage of the native pathway by the L212Gln side chain, M43Asp must activate another efficient pathway, which bypasses the L212 site, for the movement of protons to the distal carbonyl group of Q_B. Several second-site suppressor mutations that restore function to reaction centers lacking L213Asp and/or L212Glu have been characterized. In *Rb. capsulatus* and *Rb. sphaeroides*, mutation of M231Arg to Cys (*25*, *35*) can efficiently restore for the loss of L212Glu (*25*) but the rate of transfer of the second electron transfer (to which the delivery of the first proton is coupled) remains more than 25 times smaller than in the wild type (*35*). The M231 and the M43 sites are both distant from Q_B (~15 and 9−11 Å away, respectively), yet the M43Asp substitution is clearly ~25 times more effective in compensating for loss of an acidic residue at L213.

The high-resolution structures of the *Rb. sphaeroides* reaction center published by Ermler et al. (*5*) and more recently by Stowell et al. (*2*) have revealed the existence of channels of structured water molecules. One of them extends from the cytoplasm to the close vicinity of Q_B and is almost perpendicular to the membrane (*2*, *5*). The second channel is nearly parallel to the membrane (*2*). Some of the water molecules involved in the latter channel are situated at H bond distances to M44Asn (*2*) (M43 in *Rb. capsulatus*). M44Asn can also be indirectly connected to the other channel of water molecules via the side chain of L223Ser and mobile water molecules. The data of Figure 2 suggest a ≅30−40 mV negative electrostatic effect of the M43Asn → Asp mutation in the environment of Q_B; this is consistent with previous results obtained with the M43Asn → Asp single

mutant from *Rb. capsulatus* (*21*). These energetic considerations suggest that the M43Asn → Asp mutation notably increases the proton concentration in a critical part of the protein near the two water channels described above. M43Asp may also serve as an additional relay to assist in delivering protons to both proximal and distal carbonyls of Q_B, compensating in that way for the lack of L213Asp or L212Glu. The great similarity in the extent of the recoveries of the first and the second proton-transfer capabilities caused by the additional M43Asn → Asp mutation in the L213N+M44D and L212Q+M43D mutants suggests that M43 (M44 in *Rb. sphaeroides*) is in a key position to activate the transfer of both protons to Q_B, suggesting that they can use the same pathways, at least partially.

ACKNOWLEDGMENT

The authors thank Dr. L. Baciou for pertinent advice and for critical reading of the manuscript.

REFERENCES

1. Deisenhofer, J., Epp, O., Miki, K., Huber, R., and Michel, H. (1995) *J. Mol. Biol. 246*, 429−457.
2. Stowell, M. H. B., McPhillips, T. M., Rees, D. C., Soltis, S. M., Abresch, E., and Feher, G. (1997) *Science 276*, 812−816.
3. Allen, J. P., Feher, G., Yeates, T. O., Komiya, H., and Rees, D. C. (1988) *Proc. Natl. Acad. Sci U.S.A. 85*, 8487−8491.
4. Chang, C.-H., El-Kabbani, O., Tiede, D., Norris, J., and Schiffer, M. (1991) *Biochemistry 30*, 5352−5360.
5. Ermler, U., Fritzsch, G., Buchanan, S. K., and Michel, H. (1994) *Structure 2*, 925−936.
6. Arnoux, B., Gaucher, J. F., Ducruix, A., and Reiss, F. (1995) *Acta Crystallogr. D 51*, 368−379.
7. Ermler, U., Michel, H., and Schiffer, M. (1994) *J. Bioenerg. Biomembr. 26*, 5−15.
8. Leibl, W., and Breton, J. (1991) *Biochemistry 30*, 9634−9642.
9. Tiede, D. M., Vazquez, J., Cordova, J., and Marone, P. (1997) *Biochemistry 35*, 10763−10775.
10. Tiede, D. M., Utschig, L., Hanson, D. K., and Gallo, D. M. (1997) *Photosyn. Res.*, in press.
11. Okamura, M. Y., and Feher, G. (1992) *Annu. Rev. Biochem. 61*, 861−896.
12. Shinkarev, V. P., and Wraight, C. A. (1993) in *The Photosynthetic Reaction Center* (Deisenhofer, J., and Norris, J. R., Eds.) Vol. 1, pp 193−255, Academic Press, New York.
13. Sebban, P., Maróti, P., and Hanson, D. K. (1995) *Biochimie 77*, 677−694.
14. Takahashi, E., and Wraight, C. A. (1990) *Biochim. Biophys. Acta 1020*, 107−111.
15. Paddock, M. L., Rongey, S. H., McPherson, P. H., Juth, A., Feher, G., and Okamura, M. Y. (1994) *Biochemistry 33*, 734−745.
16. Maróti, P., Hanson, D. K., Baciou, L., Schiffer, M., and Sebban, P. (1994) *Proc. Natl. Acad. Sci. U.S.A. 91*, 5617−5621.
17. Rongey, S. H., Paddock, M. L., Feher, G., and Okamura, M. Y. (1993) *Proc. Natl. Acad. Sci. U. S.A. 90*, 1325−1329.
18. Hanson, D. K., Nance, S. L., and Schiffer, M. (1992) *Photosyn. Res. 32*, 147−153.
19. Hanson, D. K., Tiede, D. M., Nance, S. L., Chang, C.-H., and Schiffer, M. (1993) *Proc. Natl. Acad. Sci. U.S.A. 91*, 3034−3038.
20. Hanson, D. K., Deng, Y.-L., Sebban, P., and Schiffer, M. (1995) in *Photosynthesis: From Light to Biosphere* (Mathis, P., Ed.) Vol. I, pp 859−862, Kluwer, Dordrecht.
21. Sebban, P., Maróti, P., Schiffer, M., and Hanson, D. K. (1995) *Biochemistry 34*, 8390−8397.
22. Paddock, M. L., Rongey, S. H., Feher, G., and Okamura, M. Y. (1989) *Proc. Natl. Acad. Sci. U.S.A. 86*, 6602−6606.
23. Takahashi, E., and Wraight, C. A. (1992) *Biochemistry 31*, 855−866.
24. Shinkarev, V. P., Takahashi, E., and Wraight, C. A. (1993) *Biochim. Biophys. Acta 1142*, 214−216.
25. Miksovska, J., Kalman, L., Schiffer, M., Maróti, P., Sebban, P., and Hanson, D. K. (1997) *Biochemistry* 36, 12216−12226.
26. Youvan, D. C., Ismail, S., and Bylina, E. J. (1985) *Gene 33*, 19−30.
27. Bylina, E. J., Jovine, R. V. M., and Youvan, D. C. (1989) *Bio/Technology 7*, 69−74.
28. Miksovska, J., Maróti, P., Tandori, J., Schiffer, M., Hanson, D. K., and Sebban, P. (1996) *Biochemistry 35*, 15411−15417.
29. Simon, R., Priefer, U., and Puhler, A. (1983) *Bio/Technology 1*, 37−45.
30. Hanson, D. K., Baciou, L., Tiede, D. M., Nance, S. L., Schiffer, M., and Sebban, P. (1992) *Biochim. Biophys. Acta 1102*, 260−265.
31. Baciou, L., Bylina, E. J., and Sebban, P. (1993) *Biophysical J. 65*, 652−660.
32. Vermeglio, A. (1977) *Biochim. Biophys. Acta 459*, 516−524.
33. Wraight, C. A. (1977) *Biochim. Biophys. Acta 459*, 525−531.
34. Wraight, C. A. (1981) *Isr. J. Chem. 21*, 348−356.
35. Paddock, M. L., Senft, M. E., Graige, M. S., Rongey, S. H., Turanchik, T., Feher, G., and Okamura, M. Y. (1997) *Photosyn. Res.*, in press.

BI972696N